Research highlight

Brajesh Kumar*, Kumari Smita and Luis Cumbal

Biosynthesis of silver nanoparticles using lavender leaf and their applications for catalytic, sensing, and antioxidant activities

DOI 10.1515/ntrev-2016-0041
Received May 30, 2016; accepted June 21, 2016; previously published online September 24, 2016

Abstract: The present report summarizes an eco-friendly approach for the biosynthesis of silver nanoparticles (AgNPs) using the leaf extract of lavender. Initially, the synthesis of AgNPs was visually observed by the appearance of a wine red color. The optical property, morphology, and structure of as-synthesized AgNPs were characterized by UV-visible spectroscopy, dynamic light scattering, transmission electron microscopy, and X-ray diffraction analyses. All characterization data revealed the formation of crystalline and spherical AgNPs (Ag/Ag_2O) with size around 10–80 nm at $\lambda_{max} = 440$ nm. The surface-modified AgNPs showed an effective catalytic activity toward the reduction of 4-nitrophenol to 4-aminophenol, optical sensing of H_2O_2, and antioxidant activity against 1,1-diphenyl-2-picrylhydrazyl. The experimental approach is simple, facile, economical, and easily reproducible without any use of toxic chemicals, and opens up new scope for future biotechnology applications.

Keywords: antioxidant; biosynthesis; catalysis; sensing; silver nanoparticles; TEM; UV-vis; XRD.

1 Introduction

Lavender (*Lavandula angustifolia*) is a widely distributed herbal plant cultivated in the temperate climates of South America, Europe, and Asia. It has been traditionally considered for its very pleasant smell and bitter taste. The extract of its aerial parts and flowers contains geraniol, linalool, linalyl acetate, ursolic acid, luteolin, umbelliferone, coumarin, etc., and used in the toiletry, pharmaceutical, food, and flavor industries. It has medicinal importance in different parts of the world for the treatment of several skin sores; insect bites; pain; inflammation; burns; and gastrointestinal, nervous, and rheumatic disorders [1, 2].

In recent years, plant-derived metal nanoparticles have received special interest due to their application in various fields, including medicine, industry, agriculture, and pharmaceuticals [3]. Besides gold nanoparticles, which are the most biocompatible and chemically stable among all metal nanoparticles, silver nanoparticles (AgNPs) are preferred. Furthermore, AgNPs are economical and has shown potential applications in catalysis, nanoelectronics, optical, antibacterial, anticancer, photothermal therapy, and sensing probes for biological systems [3–5]. The advantage of plants is that they are widely distributed, easily available, much safer to handle, and serve as sources of several metabolites [6]. In this regard, biosynthesis of AgNPs using plant materials can avoid the excessive use of toxic chemicals, sophisticated instrumentations, and technical expertise; therefore, it is proving to be more economical and eco-friendly than other physical and chemical procedures [7, 8]. Thus, there is an increasing demand for green nanotechnology for the last one decade.

Nowadays, various plant materials, including *Ficus carica* fruit [9], *Lantana camara* flower [10], *Nelumbo nucifera* root [11], *Plukenetia volubilis* oil [12], *Salvadora persica* stem [13], *Nephelium lappaceum* peel [14], *Artocarpus elasticus* bark [15], and especially leaves of *Azadirachta indica* [8], *Ocimum sanctum* [16], *Aerva lanata* [17], *Coleus amboinicus* [18], *Plukenetia volubilis* [19], *Nerium oleander* [20], *Cassia tora* [21], *Camellia sinensis* [22], *Prunus yedoensis* [23], *Limonia acidissima* [24], *Rubus glaucus* [25], and *Costus pictus* [26], have been extensively used in the biosynthesis of AgNPs.

***Corresponding author: Brajesh Kumar,** Centro de Nanociencia y Nanotecnologia, Universidad de las Fuerzas Armadas ESPE, Av. Gral. Rumiñahui s/n, P.O. Box 171-5-231B, Sangolqui, Ecuador; and Department of Chemistry, TATA College, Kolhan University, Chaibasa-833202, Jharkhand, India, Tel.: +593 2 3989492, +91 8757618562, e-mail: krmbraj@gmail.com
Kumari Smita and Luis Cumbal: Centro de Nanociencia y Nanotecnologia, Universidad de las Fuerzas Armadas ESPE, Av. Gral. Rumiñahui s/n, P.O. Box 171-5-231B, Sangolqui, Ecuador

In the present work, AgNPs were synthesized using the aqueous extract of lavender leaf. The as-synthesized AgNPs were further characterized by visual inspection, UV-visible (UV-vis) spectroscopy, dynamic light scattering (DLS), transmission electron microscopy (TEM), and X-ray diffraction (XRD). These biosynthetic approaches for AgNPs also showed an effective catalytic activity for the reduction of 4-nitrophenol (4-NP) to 4-aminophenol (4-AP), optical sensing of hydrogen peroxide (H_2O_2), and antioxidant activity against 1,1-diphenyl-2- picrylhydrazyl (DPPH).

2 Experimental

2.1 Materials

Lavender leaves were collected from the local garden of Universidad de las Fuerzas Armadas ESPE, Sangolqui, Ecuador. Silver nitrate ($AgNO_3$, 99.8%), 4-nitrophenol (>99.5%), and H_2O_2 (35%) were purchased from Spectrum, USA. Sodium borohydride ($NaBH_4$, >99.5%) and DPPH (>99.5%) were purchased from Sigma Aldrich, St. Louis, MO, USA. All solutions were prepared in ultrapure Milli Q water. All chemicals were reagent grade and used without further purification.

2.2 Preparation of the extract

Thoroughly washed lavender leaves (2 g) were chopped and ultrasonicated in 25 ml of water for 3 min. After ultrasonication, the yellowish lavender leaf extract (LLE) was filtered using Whatman paper no. 1 and stored at 4°C for further use. Ultrasonication was performed with ultrasonic processors (DAIGGER GE 505, 500 W, 20 kHz) immersed directly into the reaction solution. The operating condition was at 30-s pulse on/30-s pulse off time with amplitude of 72% at 25°C for 3 min.

2.3 Biosynthesis of AgNPs

For the biosynthesis of AgNPs, 2.0 ml of LLE was completely dissolved in 20 ml of 1.0 mM $AgNO_3$ solution by vigorous stirring, and heated at 60–65°C for 30 min in the presence of visible light (55–60 cd/m^2). Reduction of Ag^+ to AgNPs occurs by the appearance of a wine red color of the reaction mixture after 3 h of incubation period, and as-synthesized AgNPs were characterized further using different analytical instruments.

2.4 Catalytic activity of AgNPs for the reduction of 4-NP to 4-AP

To test the catalytic efficacy of AgNPs, reduction of 4-NP was carried out as a model reaction and monitored as follows: about 0.2 ml of 4-NP (2 mM), 0.2 ml of as-synthesized AgNPs, and 3.4 ml of H_2O were mixed in a 4-ml standard quartz cuvette. To this reaction mixture, 0.2 ml of $NaBH_4$ (0.05 mM) solution was added and UV-vis absorption spectra were recorded at 1 min intervals, leading to a color change from pale yellow to colorless. The observed percentage of the reduction process was determined by analyzing the change in the intensity of the peaks at 400 nm as a function of time.

2.5 Optical sensing activity of AgNPs for H_2O_2

The optical sensing activity of AgNPs to detect H_2O_2 was assessed by the method adapted from Raja et al. [27], with slight modifications. In this assay, 0.5 ml of 100 mM H_2O_2 was added to 2.5 ml of diluted AgNP (5%) solution, and thoroughly mixed. The spectral absorbance was measured at regular intervals after the addition of H_2O_2.

2.6 Antioxidant activity of LLE and AgNPs

The antioxidant activity of the LLE and AgNPs was measured by using the DPPH assay adapted from Kumar et al. [9, 10], with slight modifications. The LLE/AgNPs (1000–200 µl) or control and 1000–1800 µl of H_2O were mixed with 2.0 ml of 0.2 mM DPPH in 95% ethanol. The mixture was vortexed vigorously and allowed to reach a steady state in dark incubation at room temperature for 30 min. The absorbance of the mixture was measured spectrophotometrically at 517 nm. The lower absorbance of the reaction mixture indicated a higher percentage of scavenging activity, and the percent inhibition was calculated by using the following equation:

$$\text{Scavenging activity (\%)} = \left(\frac{A_0 - A_1}{A_0}\right) \times 100, \quad (1)$$

where A_0 is the absorbance of the control (blank, without extract or AgNPs) and A_1 is the absorbance in the presence

of the LLE or AgNPs. The final result was expressed as percentage of DPPH free radical scavenging activity (ml).

2.7 Characterization of AgNPs

The synthesized AgNPs were primarily characterized with the help of a UV-vis single beam spectrophotometer (GENESYS 8; Thermo Spectronic, England). TEM and selected area electron diffraction (SAED) measurements were recorded digitally (Tecnai G2 Spirit TWIN, FEI, Holland). The samples for TEM were prepared by depositing a drop of colloidal solution on a carbon-coated copper grid and drying at room temperature. The hydrodynamic size distributions and polydispersity index (PDI) of nanoparticles were analyzed by using DLS instrumentation (LB-550; Horiba, Japan). XRD studies on thin films of the nanoparticle was carried out to identify the phase and purity, and to determine the crystallite size using a diffractometer (EMPYREAN, PANalytical) and a θ-2θ configuration (generator-detector), wherein a copper X-ray tube emitted a wavelength of λ = 1.54059 Å. The intensity data for the nanoparticle solution deposited on a glass slide were collected over a 2θ range of 5–100°. The catalytic, sensing, and antioxidant activities of AgNPs were evaluated with the help of a UV-vis spectrophotometer (SPECROD S600; Analytika Jena, Germany).

3 Results and discussion

3.1 Visual and UV-vis study

The biosynthesis of AgNPs in the colloidal solution with LLE was monitored periodically at 3, 24, 48, and 96 h by absorbance measurement using UV-vis spectroscopy and visual inspection at 96 h (Figure 1). It was observed that, in comparison with the colorless $AgNO_3$ and the pale yellow LLE, the color of the colloidal solution changed to light yellow and then wine red. It is a direct proof for the reduction of Ag^+ to Ag^0 and the formation of AgNPs. The UV-vis spectra indicated the appearance of a single surface plasmon resonance (SPR) band for the AgNPs at $\lambda_{max} = 440$ nm, which is due to the collective oscillation of the electrons in the conduction band of AgNPs [28, 29]. Also, the single SPR band for AgNPs increased with time and shifted from 440 to 460 nm. This confirms that the AgNPs have a spherical form and that the size increases with time (shift of monodisperse to polydisperse particles) [9]. Therefore, UV-vis spectra were

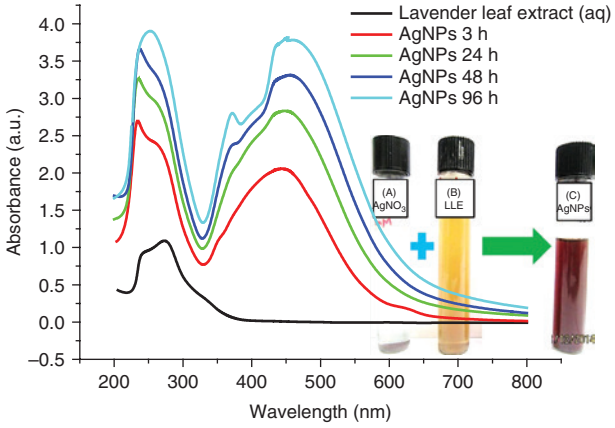

Figure 1: UV-visible absorption spectra of as-synthesized AgNPs using LLE at different incubation times at room temperature. (Inset) Visual picture of (A) 1 mM $AgNO_3$, (B) LLE, and (C) as-synthesized AgNPs after 96-h incubation at room temperature.

applied to characterize the biosynthesis of AgNPs. The difference in the standard reduction potential between Ag^+ ($E^o_{red} = +0.80$ V) and flavonoids/polyphenolic compounds present in the leaf extract ($E^o_{red} = \sim +0.3–0.8$) [30] was believed to be responsible for the reduction of Ag^+ to Ag^0 and the subsequent formation of AgNPs [Eq. (2)]. During the formation of Ag^0 in an aqueous reaction mixture, biosynthesis of Ag_2O was also suggested. It may be due to the presence of molecular oxygen (O_2) in the reaction medium, which oxidizes Ag^0 to Ag^+ and leads to the formation of Ag_2O NPs [Eq. (3)].

$$Ag^+ \text{ (aq)} + \text{flavonoids/polyphenolic (} -\text{OH, CHO, etc.)} \rightarrow Ag^0 \text{ nanoparticles (aq).} \quad (2)$$

$$Ag^0 \text{ nanoparticles (aq)} + O_2 \rightarrow Ag_2O \text{ nanoparticles (aq).} \quad (3)$$

3.2 TEM and SAED studies

The morphology, size, and crystallinity of as-synthesized AgNPs were investigated by TEM and SAED measurements. In Figure 2A,B, the TEM images indicate the formation of spherical AgNPs of diameter in the range of 10–80 nm, and that AgNPs are surrounded by LLE. The AgNPs are well separated from each other and show the absence of aggregation. This may be due to the association of LLE biomolecules on the surface of the AgNPs, and makes the surface repulsive. The observed circular white dot-like fringe patterns in SAED (Figure 2C) suggest the formation of spherical and crystalline AgNPs [31].

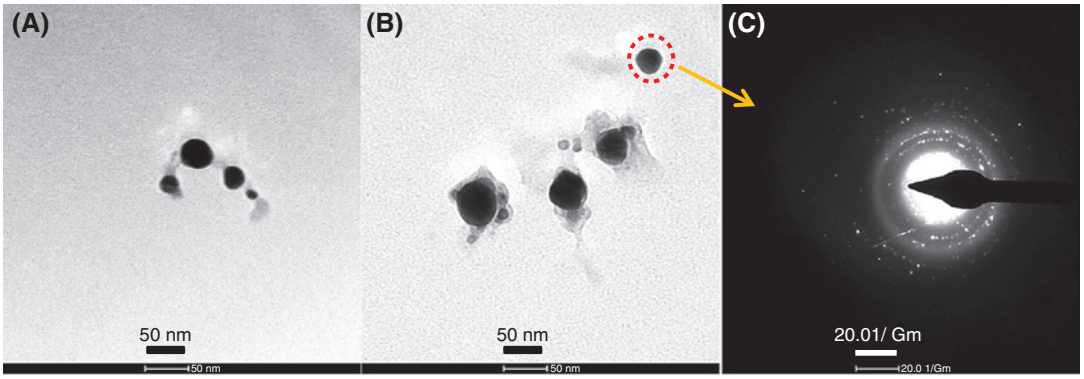

Figure 2: (A, B) TEM pictures and (C) SAED pattern of AgNPs.

3.3 DLS study

In Figure 3, the AgNPs synthesized with LLE are in the range of 20–120 nm, and the average particle size was found to be 56.9 ± 23.8 nm. The PDI of the AgNPs was 0.174, indicating a broad size distribution. The size of AgNPs observed in DLS was slightly bigger than the result obtained from TEM analysis. This may be due to the screening of smaller molecules by a bigger one and functionalization of the AgNP surface either by nitrate ions or by LLE biomolecules [14].

3.4 XRD study

It is vital to understand the exact crystal structure of the AgNPs formed, and this can be achieved by evaluating the XRD spectra of the samples. The crystalline property of AgNPs was confirmed by XRD analysis at 2θ values ranging from 5° to 100° (Figure 4). The Bragg reflection peak at 38.038° corresponds to the (111) lattice planes of face-centered cubic metallic Ag^0, which is in agreement with ICSD no. 98-018-0878. Besides the metallic Ag, another reflection peak at 32.22° corresponds to the (111) lattice planes of Ag_2O, which matched well with ICSD no. 98-003-5662. Both peaks corresponding to (111) were broad and had higher intensity than other lattice planes, suggesting the nanocrystalline nature and predominant growth of AgNPs along the (111) direction. The XRD pattern reveals that the prepared AgNPs are a mixture of metallic Ag^0 and Ag_2O.

3.5 Catalytic activity of AgNPs

To test the catalytic activity of the biosynthesized AgNPs, we studied the reduction of 4-NP to 4-AP using aqueous $NaBH_4$ by UV-vis spectroscopy. As shown in Figure 5, 4-NP shows an absorbance peak at 317 nm and 4-nitrophenolate ion in the alkaline medium (after addition of $NaBH_4$) appeared at 400 nm. The addition of $NaBH_4$ and AgNPs to the aqueous 4-NP solution produced a rapid decrease in their absorption spectra within 10 min at 400 nm with the concomitant appearance of a new peak at 298 nm indicating the formation of 4-AP. Though the reduction of 4-NP to 4-AP using aqueous $NaBH_4$ is thermodynamically favorable [E_0 for 4-NP/4-AP = −0.76 V and H_3BO_3/BH_4^- = −1.33 V vs. normal hydrogen electrode (NHE)], the presence of the kinetic barrier due to the large potential difference

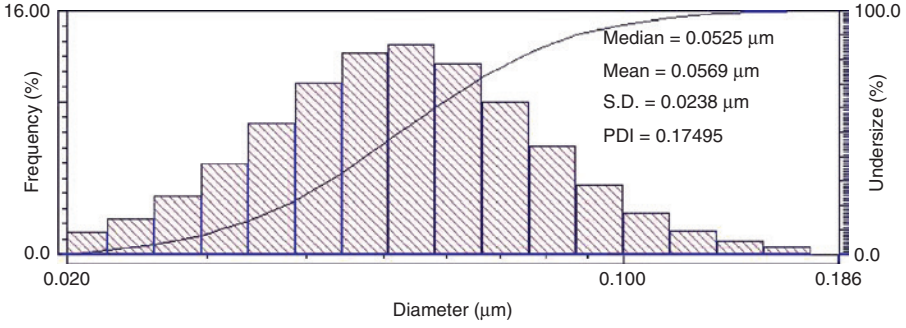

Figure 3: DLS size distribution histogram of as-synthesized AgNPs using LLE.

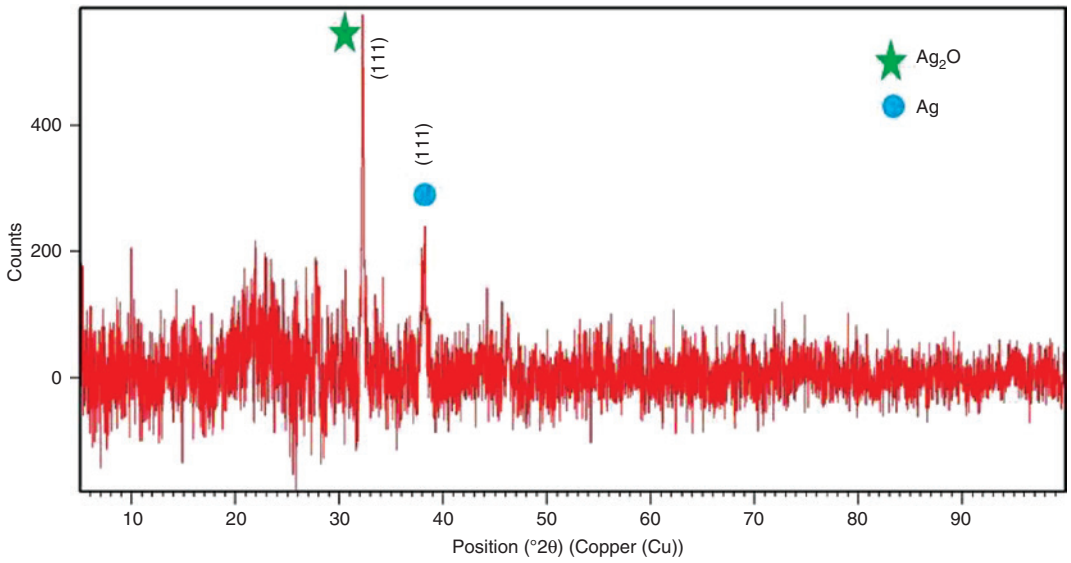

Figure 4: XRD pattern of AgNPs.

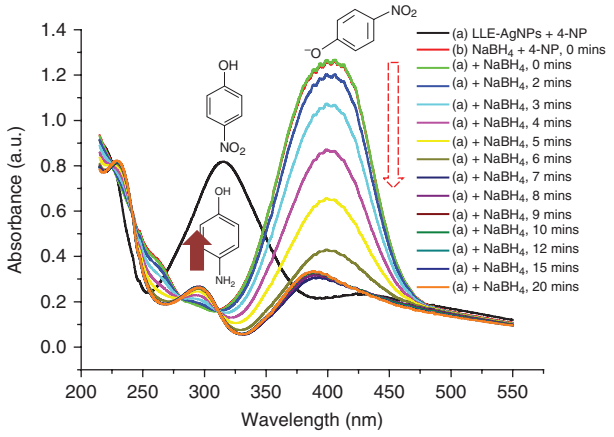

Figure 5: Catalytic activity of AgNPs for the reduction of 4-NP to 4-AP.

between donor and acceptor molecules decreased the feasibility of this reaction. It is well known that the metal nanoparticles catalyze this reaction by facilitating electron relay from the donor BH_4^- to an acceptor 4-NP to overcome the kinetic barrier. The conversion from 4-NP to 4-AP occurs via an intermediate 4-nitrophenolate ion formation, and $NaBH_4$ and AgNPs act as reducing agent and catalyst, respectively [32, 33].

3.6 Optical sensing of H_2O_2

H_2O_2 is an oxygen metabolite that induces oxidative stress and associated with aging and cancer. Moreover, H_2O_2 is widely used as a strong oxidizing agent in the food, pharmaceutical, cosmetics, wood, and pulp industries. However, the exposure to and the presence of even a small amount of H_2O_2 in process streams result in various health and environmental hazards due to its toxicity [26, 34]. The quantitative sensing of H_2O_2 has received enormous interest in the development of biosensors. Figure 6 displays the optical sensing spectra of AgNPs in the presence of H_2O_2. It shows a decreasing trend in absorbance as the time increased, and eventually the characteristic SPR peak of AgNPs at 434 nm disappeared. The maximum quenching of H_2O_2 was found to be 95% for 30 min. It is due to the spontaneous redox reaction of AgNPs with H_2O_2, and H_2O_2 can efficiently oxidize AgNPs in both acidic and basic media. The redox potential of the H_2O_2/H_2O couple (1.763 V in acidic medium) or H_2O_2/OH^- couple (0.867 V in basic medium) is higher than that of the Ag^+/Ag^0 couple (0.8 V) [35]. Thus, as-synthesized AgNP-based optical sensors for

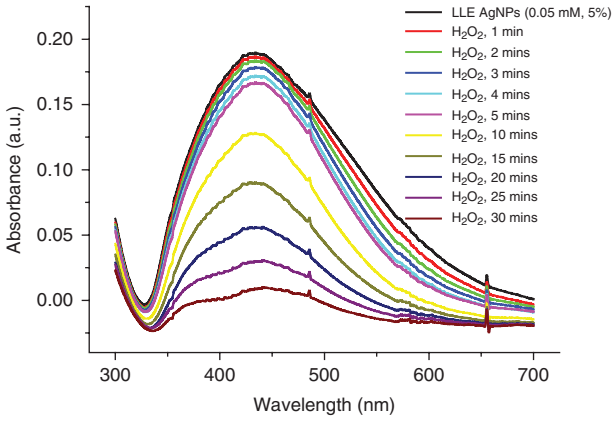

Figure 6: H_2O_2 optical sensing activity of as-synthesized AgNPs.

H_2O_2 could be potentially applied in the determination of reactive oxygen species and toxic chemicals.

3.7 Antioxidant activity

Polyphenols and their modified nanoparticles have powerful antioxidant activity and are capable of scavenging a wide range of free radicals [7, 25]. The evaluation of the antioxidant activity of LLE and AgNPs by the DPPH method is shown in Figure 7. It could be noted that the DPPH scavenging activity for LLE and AgNPs increases in a dose-dependent manner. At lower concentrations, the scavenging activity of AgNPs (5.33%, 0.1 ml; 12.91%, 0.2 ml; 29.5%, 0.4 ml; 35.18%, 0.6 ml; and 34.95%, 0.8 ml) was higher than that of LLE (1.83%, 0.1 ml; 4.73%, 0.2 ml; 7.70%, 0.4 ml; 14.09%, 0.6 ml; and 22.27%, 0.8 ml), whereas, at 1 ml concentration, it is 27.48% and 34.28% for AgNPs and LLE, respectively. It is due to the synergistic result of an active physicochemical interaction of Ag atoms with the functional groups of the LLE and, at higher concentration, less solubility of AgNPs [14, 19].

4 Conclusions

The study demonstrated a promising, low-cost, and eco-friendly method to synthesize AgNPs by using LLE. The phytochemicals present in lavender leaf cause the bioreduction of Ag^+ to their metallic forms. The evaluation of AgNPs by UV-vis spectroscopy demonstrates that the AgNPs formed are nanosized and have an SPR peak at 440 nm. The TEM and DLS results revealed that the synthesized AgNPs were spherical with size around 10–80 nm. The XRD pattern reveals that the prepared AgNPs are a mixture of metallic Ag and Ag_2O. Finally, this finding suggests that the eco-friendly biosynthesized AgNPs have proven to be promising catalysts, sensors, and antioxidants.

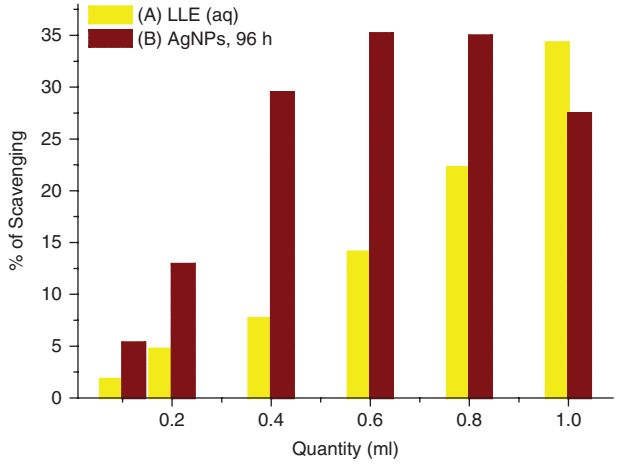

Figure 7: Antioxidant activity of (A) LLE and (B) AgNPs after 96 h.

Acknowledgments: This scientific work has been funded by the Universidad de las Fuerzas Armadas ESPE and Prometeo Project of the National Secretariat of Higher Education, Science, Technology and Innovation (SENESCYT), Ecuador. We also thank Dr. Alexis Debut, ESPE, for providing the TEM and XRD facilities.

Conflict of interest statement: The authors confirm they have no conflict of interests.

References

[1] Hajhashemi V, Ghannadi A, Sharif B. Anti-inflammatory and analgesic properties of the leaf extracts and essential oil of *Lavandula angustifolia* Mill. *J. Ethnopharmacol.* 2003, 89, 67–71.
[2] Jivad N, Rabiei Z. A review study on medicinal plants used in the treatment of learning and memory impairments. *Asian Pac. J. Trop. Biomed.* 2014, 4, 780–789.
[3] Mohammadinejad R, Karimi S, Iravani S, Varma RS. Plant-derived nanostructures: types and applications. *Green Chem.* 2016, 18, 20–52.
[4] Leite PEC, Pereira MR, Granjeiro JM. Hazard effects of nanoparticles in central nervous system: searching for biocompatible nanomaterials for drug delivery. *Toxicol. In Vitro* 2015, 29, 1653–1660.
[5] Cuenya BR. Synthesis and catalytic properties of metal nanoparticles: size, shape, support, composition, and oxidation state effects. *Thin Solid Films* 2010, 518, 3127–3150.
[6] Balaprasad A, Damle C, Ahmad A, Murali S. Biosynthesis of gold and silver nanoparticles using *Emblica officinalis* fruit extract, their phase transfer and trans metallation in an organic solution. *J. Nanosci. Nanotechnol.* 2005, 5, 1665–1671.
[7] Kumar B, Smita K, Cumbal L, Camacho J, Hernández-Gallegos E, Chávez-López MG, Grijalva M, Andrade K. One pot phytosynthesis of gold nanoparticles using *Genipa americana* fruit extract and its biological applications. *Mater. Sci. Eng. C* 2016, 62C, 725–731.
[8] Shankar SS, Rai A, Ahmad A, Sastry M. Rapid synthesis of Au, Ag, and bimetallic Au core-Ag shell nanoparticles using Neem (*Azadirachta indica*) leaf broth. *J. Colloid Interface Sci.* 2004, 275, 496–502.
[9] Kumar B, Smita K, Cumbal L, Debut A. *Ficus carica* (fig) fruit mediated green synthesis of silver nanoparticles and its antioxidant activity: a comparison of thermal and ultrasonication approach. *BioNanoSci* 2016, 6, 15–21.
[10] Kumar B, Smita K, Cumbal L. Biosynthesis of silver nanoparticles using *Lantana camara* flower extract and its application. *J. Sol-Gel Sci. Technol.* 2016, 78, 285–292.

[11] Sreekanth TVM, Ravikumar S, Eom IY. Green synthesized silver nanoparticles using *Nelumbo nucifera* root extract for efficient protein binding, antioxidant and cytotoxicity activities. *J. Photochem. Photobiol. B Biol.* 2014, 141, 100–105.
[12] Kumar B, Smita K, Cumbal L, Debut A. Sacha inchi (*Plukenetia volubilis* L.) oil for one pot synthesis of silver nanocatalyst: an ecofriendly approach. *Ind. Crops Prod.* 2014, 58, 238–243.
[13] Tahir K, Nazir S, Li B, Khan AU, Khan ZUH, Ahmad A, Khan FU. An efficient photo catalytic activity of green synthesized silver nanoparticles using *Salvadora persica* stem extract. *Sep. Purif. Technol.* 2015, 150, 316–324.
[14] Kumar B, Smita K, Angulo Y, Cumbal L. Valorization of rambutan peel for the synthesis of silver-doped titanium dioxide (Ag/TiO_2) nanoparticles. *Green Process. Synt.* 2016, 5, 371–377.
[15] Abdullah NISB, Ahmad MB, Shameli K. Biosynthesis of silver nanoparticles using *Artocarpus elasticus* stem bark extract. *Chem. Central J.* 2015, 9, 61.
[16] Singhal G, Bhavesh R, Kasariya K, Sharma AR, Singh RP. Biosynthesis of silver nanoparticles using *Ocimum sanctum* (Tulsi) leaf extract and screening its antimicrobial activity. *J. Nanopart. Res.* 2011, 13, 2981–2988.
[17] Joseph S, Mathew B. Microwave assisted facile green synthesis of silver and gold nanocatalysts using the leaf extract of *Aerva lanata*. *Spectrochim. Acta Pt. A Mol. Biomol. Spectrosc.* 2015, 136, 1371–1379.
[18] Narayanan KB, Sakthivel N. Extracellular synthesis of silver nanoparticles using the leaf extract of *Coleus amboinicus* Lour. *Mater. Res. Bull.* 2011, 46, 1708–1713.
[19] Kumar B, Smita K, Cumbal L, Debut, A. Synthesis of silver nanoparticles using Sacha inchi (*Plukenetia volubilis* L.) leaf extracts. *Saudi J. Biol. Sci.* 2014, 21, 605–609.
[20] Tahir K, Nazir S, Li B, Khan, Khan ZUH, Gong PY, Khan SU, Ahmad A. *Nerium oleander* leaves extract mediated synthesis of gold nanoparticles and its antioxidant activity. Mater. Lett. 2015, 156, 198–201.
[21] Saravanakumar A, Ganesh M, Jayaprakash J, Jang HT. Biosynthesis of silver nanoparticles using *Cassia tora* leaf extract and its antioxidant and antibacterial activities. *J. Ind. Eng. Chem.* 2015, 28, 277–281.
[22] Nestor ARV, Mendieta VS, Lopez MAC, Espinosa RMG, Lopez MAC, Alatorre JAA. Solventless synthesis and optical properties of Au and Ag nanoparticles using *Camiellia sinensis* extract. *Mater. Lett.* 2008, 62, 3103–3105.
[23] Velmurugan P, Cho M, Lim S-S, Seo S-K, Myung H, Bang K-S, Sivakumar S, Cho K-M, Oh B-T. Phytosynthesis of silver nanoparticles by *Prunus yedoensis* leaf extract and their antimicrobial activity. *Mater. Lett.* 2015, 138, 272–275.
[24] Annavaram V, Posa VR, Uppara VG, Jorepalli S, Somala AR. Facile green synthesis of silver nanoparticles using *Limonia acidissima* leaf extract and its antibacterial activity. *BioNanoSci* 2015, 5, 97–103.
[25] Kumar B, Smita K, Seqqat R, Benalcazar K, Grijalva M, Cumbal L. *In vitro* evaluation of silver nanoparticles cytotoxicity on hepatic cancer (Hep-G2) cell line and their antioxidant activity: green approach for fabrication and application. *J. Photochem. Photobiol. B Biol.* 2016, 159, 8–13.
[26] Nakkala JR, Bhagat E, Suchiang K, Sadras SR. Comparative study of antioxidant and catalytic activity of silver and gold nanoparticles synthesized from *Costus pictus* leaf extract. *J. Mater. Sci. Technol.* 2015, 31, 986–994.
[27] Raja S, Ramesh V, Thivaharan V. Green biosynthesis of silver nanoparticles using *Calliandra haematocephala* leaf extract, their antibacterial activity and hydrogen peroxide sensing capability. *Arab. J. Chem.* 2015, in press, Available at: http://dx.doi.org/10.1016/j.arabjc.2015.06.023. Accessed 27 June, 2015.
[28] Mulvaney P. Surface plasmon spectroscopy of nanosized metal particles. *Langmuir* 2006, 12, 788–800.
[29] Agasti N, Kaushik NK. Myristic acid capped silver nanoparticles: aqueous phase synthesis and pH-induced optical properties. *J. Chin. Adv. Mater. Soc.* 2014, 2, 31–39.
[30] Huang L, Weng X, Chen Z, Megharaj M, Naidu R. Green synthesis of iron nanoparticles by various tea extracts: comparative study of the reactivity. *Spectrochim. Acta Pt. A* 2014, 130, 295–301.
[31] Das SK, Khan MR, Parandhaman T, Laffir F, Guha AK, Sekaran G, Mandal AB. Nano-silica fabricated with silver nanoparticles: antifouling adsorbent for efficient dye removal, effective water disinfection and biofouling control. *Nanoscale* 2013, 5, 5549–5560.
[32] Pradhan N, Pal A, Pal T. Silver nanoparticle catalyzed reduction of aromatic nitro compounds. *Colloids Surf. A Physicochem. Eng. Aspects* 2002, 196, 247–257.
[33] Gangula A, Podila R, Karanam RML, Janardhana C, Rao AM. Catalytic reduction of 4-nitrophenol using biogenic gold and silver nanoparticles derived from *Breynia rhamnoides*. Langmuir 2011, 27, 15268–15274.
[34] Bera RK, Raj CR. A facile photochemical route for the synthesis of triangular Ag nanoplates and colorimetric sensing of H_2O_2. *J. Photochem. Photobiol. A Chem.* 2013, 270, 1–6.
[35] Zhang Q, Cobley CM, Zeng J, Wen L-P, Chen J, Xia Y. Dissolving Ag from Au-Ag alloy nano boxes with H_2O_2: a method for both tailoring the optical properties and measuring the H_2O_2 concentration. *J. Phys. Chem. C* 2010, 114, 6396–6400.

Bionotes

Brajesh Kumar
Centro de Nanociencia y Nanotecnologia, Universidad de las Fuerzas Armadas ESPE, Av. Gral. Rumiñahui s/n, P.O. Box 171-5-231B, Sangolqui, Ecuador; and Department of Chemistry, TATA College, Kolhan University, Chaibasa-833202, Jharkhand, India, Tel.: +593 2 3989492, +91 8757618562
krmbraj@gmail.com

Brajesh Kumar is currently working as a Prometeo investigator/visiting professor at the Centro de Nanociencia y Nanotecnologia, Universidad de las Fuerzas Armadas ESPE, Ecuador. He received his MSc and PhD in chemistry from the University of Delhi, India. His research interest is in the development of sustainable and eco-friendly technique for the synthesis of different nanoparticles/nanocomposites and their applications for environmental remediation, nanomedicine, sensors, organic synthesis, active films of organic solar cells, etc.

Kumari Smita
Centro de Nanociencia y Nanotecnologia,
Universidad de las Fuerzas Armadas ESPE,
Av. Gral. Rumiñahui s/n, P.O. Box 171-5-231B,
Sangolqui, Ecuador

Kumari Smita completed her master's degree in inorganic chemistry at Ranchi University, India. She worked as a senior research assistant at the National Metallurgical Laboratory (NML), Jamshedpur, India, for 6 years and has been associated with Centro de Nanociencia y Nanotecnologia for the last 3 years. Her current research interest is focused on the development of green and sustainable processes for the synthesis of nanoparticles, nanocomposites, and remediation of organic dyes, heavy metal ions, etc.

Luis Cumbal
Centro de Nanociencia y Nanotecnologia,
Universidad de las Fuerzas Armadas ESPE,
Av. Gral. Rumiñahui s/n, P.O. Box 171-5-231B,
Sangolqui, Ecuador

Luis Cumbal received his PhD from Lehigh University, USA. He has been dedicated to researching and developing new materials to be applied in the environmental remediation of soils and water. Currently, Dr. Cumbal is the director of the Center for Nanoscience and Nanotechnology and professor at the Department of Life Sciences at the Universidad de las Fuerzas Armadas, Ecuador.